Performance assessment and cycle layout identification of Brayton cycle heat pumps for combined heat and cold production: a heat pump superstructure approach

Christophe Vankelekom[a], Panagiotis Stathopoulos[b] and Ward De Paepe[a,c,d]

[a] *University of Mons (UMONS), Mons, Belgium, christophe.vankelekom@umons.ac.be CA*
[b] *German Aerospace Centre (DLR), Cottbus, Germany, panagiotis.stathopoulos@dlr.de*
[c] *UMONS Micro-gAsturbine Research Centre-UMARC, Mons, Belgium, Ward.DEPAEPE@umons.ac.be*
[d] *WEL Research Institute, Wavre, Belgium, Ward.DEPAEPE@umons.ac.be*

Abstract:
Achieving the net-zero objective by 2050 requires not only a shift to renewable electricity but also the electrification of industrial heat processes. In Europe, industry accounts for about 25% of total energy demand, with nearly 66% of this energy required for process heat, which is still mainly produced by the combustion of fossil fuels. To defossilize this sector, air-based reverse Brayton cycle (RBC) heat pumps offer a promising alternative. This technology enables reaching high temperatures above 200 °C, but it typically has a low Coefficient of Performance (COP) as gas is used as a working medium. This disadvantage can be mitigated by valorising the cooling available at the heat source, thus increasing the overall COP. Although interest in Brayton cycle heat pumps has recently grown, there is still a lack of systematic analysis to evaluate the thermodynamic potential limits regarding their performance over a wide range of operating conditions and which cycle configuration should be selected. Therefore, this work addresses this gap by exploring this technology for combined heating and cooling production using a heat pump superstructure approach. The model is optimised for various operating conditions with variations of heat source and heat sink temperatures. From this analysis, the recuperated RBC layout is the optimal configuration under most operating conditions, reaching heating and total COP values up to 1.37 and 1.85. However, for a sufficiently high heat source inlet temperature and low heat sink inlet temperatures, the basic RBC layout performs better, with heating and total COP up to 1.85 and 2.82. In all cases, COP decreases as the heat sink inlet temperature rises. The system compensates by reducing the working mass flow rate and increasing the compressor outlet temperature, which may lead to potential technical limitations due to higher pressure ratios.

Keywords:
Brayton cycle, Heat pump superstructure, Heating and cooling, Thermodynamic, MINLP.

1. Introduction

In Europe, industry is responsible for approximately 25% of total energy demand, with about 66% of this energy required for process heating [1]. Unfortunately, the heating sector still mainly relies on fossil fuels to reach high temperatures. Industrial heat demand can be classified into three main categories: Low (below 150°C), medium (150°C-400°C) and high (above 400°C), representing 30%, 22% and 48% of the demand, respectively [2]. To defossilize these sectors, the heat pump system has been identified as a promising candidate. This technology is already well established for the low-temperature applications, mainly covered by vapour compression cycle heat pumps, achieving a Coefficient of Performance (COP) between 2.5 and 4 for supplying heat between 120°C and 160°C [3].

However, for temperatures above 200°C, vapour compression cycles suffer from several limitations, such as lubricant issues, challenging fluid selection (high-pressure ratio and thermal stability), and

waste heat usage for techno-economic feasibility [4,5]. To overcome previous limitations, the reverse Brayton cycle has been identified as a promising option. Indeed, it has been identified as a simple construction for large temperature glide while producing heat at high temperatures above 400 °C [6]. In addition, natural working fluids are used, such as air, argon, and helium, which exhibit zero ozone depletion potential, zero global warming potential, and no flammability limits, while also offering satisfactory thermodynamic properties for high-temperature applications [7]. However, Brayton heat pumps typically exhibit a low COP compared to vapour compression cycles [8, 9] due to the use of gas as a working medium. To mitigate this limitation, cooling available at the heat source can be valorised to enhance the overall performance of the heat pump. This simultaneous production is particularly beneficial for industrial processes that require both high-temperature heat above 150 °C and low-temperature cooling between -30 °C and 5 °C. These demands are mostly found within the food, beverage and tobacco industry, characterised by a thermal heating power below 1 MW_{th} [3, 10, 11].

Despite this potential, only a limited number of studies have investigated the combined use of RBC heat pumps for simultaneous heating and cooling. Among them, one study [12] investigated 9 cycle configurations for a given heat sink setup, with inlet and outlet temperatures of 100 °C and 250 °C, respectively, and a thermal heating power of 150 kWth. For each configuration, the COP was optimised for different heat source outlet temperatures. Several layouts were found to achieve a total COP (accounting for heating and cooling production) above 2, and a heating COP around 1.5. They concluded that among all the architectures, recuperated cycles are preferred as soon as simultaneous heating and cooling at a low temperature (-30°C to-15°C) is desired. Furthermore, cycles with inter-cooling and inter-heating between compressors and turbines can be advantageous when high pressure ratios and low heat source outlet temperatures are needed. Their analysis was based on the CoBra pilot plant, which serves as a reference process architecture for defining modelling parameters and boundary conditions. Developed by the German Aerospace Centre, the CoBra pilot plant [13] is an experimental facility used for testing and piloting of RBC. It has provided the necessary proof of concept and commissioning of the technology. The CoBra test rig shows the possibility of reaching a compressor outlet temperature of 260 °C and a turbine outlet temperature of -30 °C simultaneously [13].

Nevertheless, there is still a lack of fundamental studies related to Brayton cycle heat pumps that systematically assess their potential in terms of performance while identifying the optimal cycle layout for combined heating and cooling applications. Thus, in this work, we aim to develop such a framework for the systematic characterisation of Brayton cycles to get a deeper fundamental understanding. For that purpose, a heat pump superstructure model is used. This superstructure model is composed of a stage-wise superstructure approach for the heat exchanger network synthesis and mathematical formulation for the radial turbomachinery. This model is formulated as a pseudo Mixed Integer Non-Linear Programming (MINLP) problem. Similar approaches have previously been applied to the optimal integration of vapour compression heat pumps into industrial processes, either through advanced pinch analysis methods [14] or also via superstructure heat pump-based formulation [15]. However, such methodologies have not yet been extended to Brayton cycle heat pumps, particularly in the context of combined heating and cooling production.

In this paper, the objective is to evaluate the influence of changing the operating conditions on the COP, the impact on the temperature levels within the Brayton cycle, the maximum achievable thermal cooling production, and the potential technical limitations of the system, while identifying the optimal cycle layout. For that purpose, the considered heat pump consists of a single-stage compression and a single-stage expansion, which is optimised for two heat source temperatures (5 °C and 70 °C), corresponding respectively to a closed cooling loop and the recovery of waste heat from the industrial process. For each scenario, three heat sink outlet temperatures are investigated (200 °C, 250 °C and 300 °C) while varying the heat sink inlet temperature. The required thermal heating power is fixed to

150 kW_{th}. This paper is structured into two main parts. The first part is related to the methodology applied, including mathematical formulations, assumptions and operating conditions considered. The second part discusses the results, mainly focusing on the performance, temperature levels, cooling capacity and the identification of optimal cycle configurations under different operating conditions.

2. Methodology

This section is divided into four main parts. First, the working principle of the RBC heat pump is rapidly presented. Second, the working principle of the heat pump superstructure is detailed. The latter sub-section is followed by the modelling of the system. Finally, the considered operating conditions and assumptions will be provided in the last sub-section.

2.1. Brayton cycle heat pump

The reverse Brayton cycle heat pump considered in this study operates in a closed loop in which dry air is flowing (79% nitrogen and 21% oxygen, by molar fraction). The simplest configuration (Fig. 1) consists of a compressor, a turbine and two heat exchangers. First, air initially at atmospheric pressure (state 1) is compressed, leading to an increase in temperature (state 2). It then transfers heat to the heat sink before being expanded in the turbine (state 3). The expansion process enables partial recovery of the compressor work, thereby reducing the net electrical power consumption. Depending on the operating conditions, the turbine outlet temperature (state 4) may reach sufficiently low values to valorise the cooling production available at the heat source. More advanced configurations may include multiple compressors, turbines and heat exchangers to enhance the overall performance of the heat pump. This could be determined during the optimisation process as the identification of the optimal layout is carried out simultaneously.

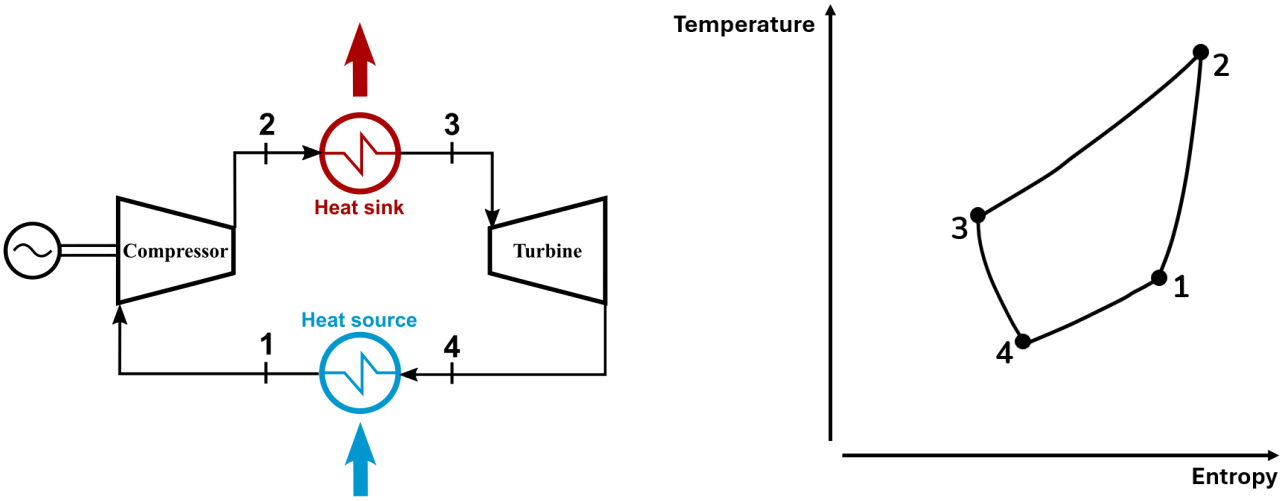

Figure 1: Basic Brayton cycle heat pump (a) and its corresponding T-s diagram (b).

2.2. Heat pump superstructure

The heat pump superstructure approach constitutes an interesting alternative to conventional design methodologies. Rather than predefining a set of cycle configurations and optimising each of them with respect to selected parameters, this approach starts from a large superstructure that gathers multiple possible layouts. For given operating conditions, the optimisation framework simultaneously evaluates the maximum heat pump performance and identifies the optimal cycle layout that decreases heat exchanger network complexity. Therefore, the heat pump superstructure model combines mathematical formulations describing the behaviour of turbomachinery (e.g., compressors and turbines) with a heat exchanger network represented using a stage-wise superstructure approach, originally pro-

posed by Yee and Grossmann [16]. This method shares similarities with pinch analysis, introduced by Linnhoff and Flower [17], which aims to minimise energy consumption from external hot and cold utilities while satisfying a minimum temperature difference (pinch) for economic feasibility.

However, the stage-wise superstructure approach comes with a higher computational cost compared to pinch analysis methods because it explicitly considers all possible heat exchanger matches. This cost increases strongly with the number of streams and stages considered. To limit this complexity, the present study focuses on a simplified system with a single compressor and turbine, and fixed heat sink and heat source conditions. This serves as a test case before extending the approach to more complex configurations and assessing the full potential of RBC heat pumps.

The considered system and its working principle are shown in Fig. 2. In this framework, each stream is divided into a user-specified number of stages within which heat exchange between hot and cold streams can occur. Hot streams are directed from left to right, while cold streams are oriented from right to left to simulate counter-current heat exchange. The number of stream splits is determined according to the number of opposite stream types, enabling all feasible matches.

For the simplified system, two hot streams and two cold streams are considered, as indicated by heaters (red) or coolers (blue) in Fig.2. The hot streams correspond to the heat source and the compressed air stream between the compressor outlet and the turbine inlet. The cold streams include the heat sink and the expanded air stream between the turbine outlet and the compressor inlet. Components and streams of the heat pump are in the green area shown in the figure. The heat source and heat sink streams represent the industrial demand and are completely covered by the heat pump, as no external hot and cold utilities are considered in this study.

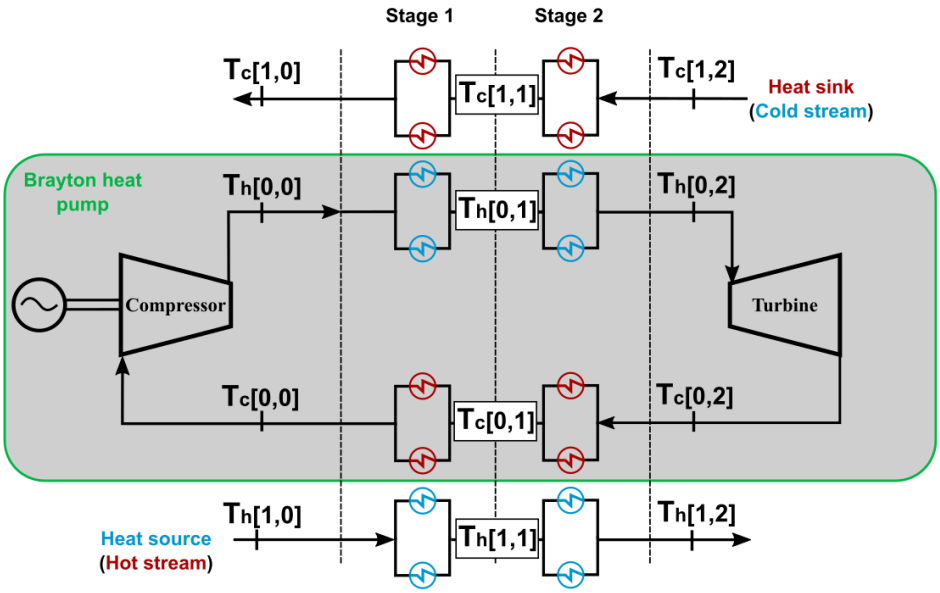

Figure 2: Heat pump superstructure model used to optimise heat pump performance (grey box) and identify optimal cycle configuration for the heat exchanger network.

2.3. System modelling

The heat pump superstructure model includes both continuous variables (e.g., temperatures and heat duties) and binary variables, which are used to activate or deactivate heat exchangers and identify stream matches within each stage. The formulation comprises heat balance equations at both stage and stream levels, logical and feasibility constraints, and surrogate models for the compressor, turbine and enthalpy calculations. Due to the combination of non-linear relationships and binary numbers,

the resulting problem is formulated as a Mixed Integer Non-Linear Programming (MINLP) model. To implement the different equation that constitutes this model, the indices i,j and k are used to differentiate hot streams, cold streams and stages, respectively. In Fig. 2, the subscripts h (hot) and c (cold) are used for clarity. The number of stages (N_{stages}) is specified a priori to have sufficient flexibility. For a system with k stages, k+1 temperature nodes are defined, as illustrated in Fig. 2. Equations for heat balances, logical and feasibility constraints, are presented below in three categories: heat pump, thermal balance, and feasibility constraints. Then, the objective function for the optimisation is detailed.

2.3.1. Heat pump

The heat pump components mainly consist of the compressor and turbine, which link cold and hot stream temperatures at the boundaries of the superstructure (i.e., inlet and outlet stages). In this formulation, the heat pump streams are indexed by i and j equal to 0, while i,j = 1 correspond to the external heat sink and heat source streams, as shown in Fig. 2. Both compressor and turbine are represented through a surrogate model, defined by the functions $F_{comp}(T_{in}, \pi_{comp})$ and $F_{turb}(T_{in}, 1/\pi_{comp})$, which provides the outlet temperature as a function of inlet temperature (T_{in}) and pressure ratio (π_{comp}). These surrogate models are derived from a database generated with Aspen Plus software [18]. The dataset covers inlet temperatures ranging from -20 to 200 °C (1 °C step) and pressure ratios from 1 to 6 (0.1 step), assuming constant isentropic efficiency for both components. The corresponding turbomachinery equations are thus:

$$T_h[0,0] = F_{comp}(T_c[0,0], \pi_{comp}), \tag{1}$$

$$T_c[0, N_{stages}] = F_{turb}(T_h[0, N_{stages}], 1/\pi_{comp}). \tag{2}$$

As this heat pump is a closed loop, the mass flow rate of the hot and cold streams must be equal ($\dot{m}_h[0] = \dot{m}_c[0]$).

2.3.2. Thermal balance

Two types of heat balance equations are considered. The first set describes the temperature evolution of hot and cold within each stage due to heat exchange:

$$(h_h[i,k] - h_h[i,k+1])\dot{m}_h[i] = \sum_j Q[i,j,k]\, Z[i,j,k], \tag{3}$$

$$(h_c[j,k] - h_c[j,k+1])\dot{m}_c[j] = \sum_i Q[i,j,k]\, Z[i,j,k]. \tag{4}$$

Here, $h_{h/c}$ is the enthalpy of the hot and cold streams, respectively, computed using a surrogate model (F_h(T,p)), similar to those used for the compressor and turbine. The inputs are temperature and pressure, which correspond to the atmospheric pressure (BP) or high-pressure (HP = BP pi_c). The high-pressure only applies to the hot stream in the RBC heat pump (i=0). Q represents the thermal power exchanged between hot and cold streams, while Z is the binary variable defining the stream matches. The second set of equations ensures the overall thermal balance of each stream across all stages:

$$(h_h[i,0] - h_h[i,N_{stages}])\dot{m}_h[i] = \sum_k \sum_j Q[i,j,k]\, Z[i,j,k], \tag{5}$$

$$(h_c[j,0] - h_c[j,N_{stages}])\dot{m}_c[j] = \sum_k \sum_i Q[i,j,k]\, Z[i,j,k]. \tag{6}$$

As previously stated, the inlet and outlet temperatures of the heat sink and heat source streams are imposed by industrial requirements. However, only the thermal load of the heat sink is specified

so that the influence of the operating conditions on the thermal cooling production can be analysed. Consequently, the imposed mass flow rate ($\dot{m}_c[1]$) corresponds to the heat capacity flow rate. Thus, (3) to (6) use temperatures instead of enthalpies.

2.3.3. Feasibility/logical constraints

To prevent temperature crossovers between streams, an Exchanger Minimum Approach Temperature (EMAT) is implemented by the following constraints:

$$\Delta T_{\text{EMAT}} \leq (T_{\text{h}}[i,k] - T_{\text{c}}[i,k]) + \alpha(1 - Z[i,j,k]), \tag{7}$$

$$\Delta T_{\text{EMAT}} \leq (T_{\text{h}}[i,k+1] - T_{\text{c}}[i,k+1]) + \alpha(1 - Z[i,j,k]). \tag{8}$$

Here, ΔT_{EMAT} is the minimum allowable temperature difference (pinch) in the heat exchanger network. The term $\alpha(1 - Z[i,j,k])$ acts as a bypass, ensuring that the constraint is ignored when a hot stream temperature is below a cold stream temperature, implying no possible matches [16]. The parameter α is chosen sufficiently large (e.g., equal to 400) to ensure this behaviour. Furthermore, two additional constraints are introduced to ensure that the compressor and turbine outlet temperatures meet the heat sink and heat source requirements, respectively:

$$T_{\text{h}}[0,0] \geq T_{\text{sink,out}} + \Delta T_{\text{EMAT}}, \tag{9}$$

$$T_{\text{c}}[0, N_{\text{stages}}] \leq T_{\text{source,out}} - \Delta T_{\text{EMAT}}. \tag{10}$$

2.3.4. Objective function and simulations

The objective of the optimisation is to minimise the difference between the number of heat exchangers and the total Coefficient of Performance (COP_{tot}) of the heat pump:

$$f_{\text{Obj}} = N_{\text{HX}} - COP_{\text{tot}}. \tag{11}$$

Although alternative formulations with normalised COP with the Carnot COP or weights could be used, this was not considered necessary for the simplified case considered, as both terms are of the same order of magnitude for the operating conditions investigated. Typical total COP values range between 1.5 and 2.5, while the number of heat exchangers varies between 2 and 4. Therefore, the chosen objective provides a simple way to balance system complexity and thermodynamic performance without introducing weighting factors or detailed cost correlations, which are highly non-linear. The COP_{tot} is computed as follows:

$$COP_{\text{tot}} = \frac{Q_{\text{heating}} + Q_{\text{cooling}}}{P_{\text{comp}} + P_{\text{turb}}} \tag{12}$$

As already discussed, the resulting formulation leads to a MINLP problem. Such problems are challenging to solve due to their non-convexity and strong non-linearities. To mitigate this complexity and reduce computational effort, the MINLP is decomposed into a set of Non-Linear Programming (NLP) subproblems by fixing the binary variable Z, which is not known a priori. For a system with two stages and four streams, there are 16 heat exchangers, corresponding to 8 different values of the vector Z and thus 2^8 (256) possible combinations. This number rapidly increases with the number of stages and streams. For that reason, given that the system consists of two hot and two cold streams, at least two heat exchangers are required. To limit computational cost, an upper bound of 4 heat exchangers is fixed, which drastically reduces the number of possible combinations. The resulting NLPs are solved independently in parallel to further accelerate computations. Finally, (1)-(10) have been implemented in the open-source Casadi framework for non-linear optimisation [19] and the NLP problems are solved using the ipopt solver, which is a high-performance open-source solver [20].

2.4. Heat pump operating conditions

The proposed heat pump superstructure model is optimised over a wide range of operating conditions. Two heat source scenarios are analysed. First, a low heat source inlet temperature of 5 °C is selected to simulate a closed-loop cooling process, meaning that the outlet temperature of the cooling process corresponds to the heat source inlet temperature. Second, a higher heat source inlet temperature of 70 °C is chosen to represent the utilisation of waste heat from the process. For both scenarios, the heat source outlet temperature is fixed at -15 °C. Three heat sink outlet temperatures are also investigated, namely 200 °C, 250 °C and 300 °C. For each case, the heat sink inlet temperature is varied from 15 °C to 180 °C to modify the temperature glide within the heat sink. The required thermal heating power is fixed at 150 kW_{th}. Regarding the turbomachinery, radial components are assumed, as this study targets sub-MW_{th} applications. For these components, constant isentropic efficiencies of 80% and 85% are selected for the compressor and turbine, respectively, while imposing an electro-mechanical efficiency of 95% for both machines [12, 21]. The low-pressure level of the heat pump is fixed at atmospheric pressure (101,325 Pa) while a maximum pressure ratio of 6 has been selected. The turbine outlet temperature is limited to - 60 °C to prevent freezing issues. For the heat exchanger network synthesis, an EMAT value of 15 °C is imposed, and the number of stages is set to three.

3. Results

This section presents the results obtained for the two heat source scenarios, corresponding to inlet temperatures of 5 °C (scenario 1) and 70 °C (scenario 2). With the exception of the figures showing the working mass flow rate, thermal cooling power and compressor pressure ratio, all plots follow a consistent layout, where results for scenario 1 are shown on the left-hand side and scenario 2 on the right-hand side.

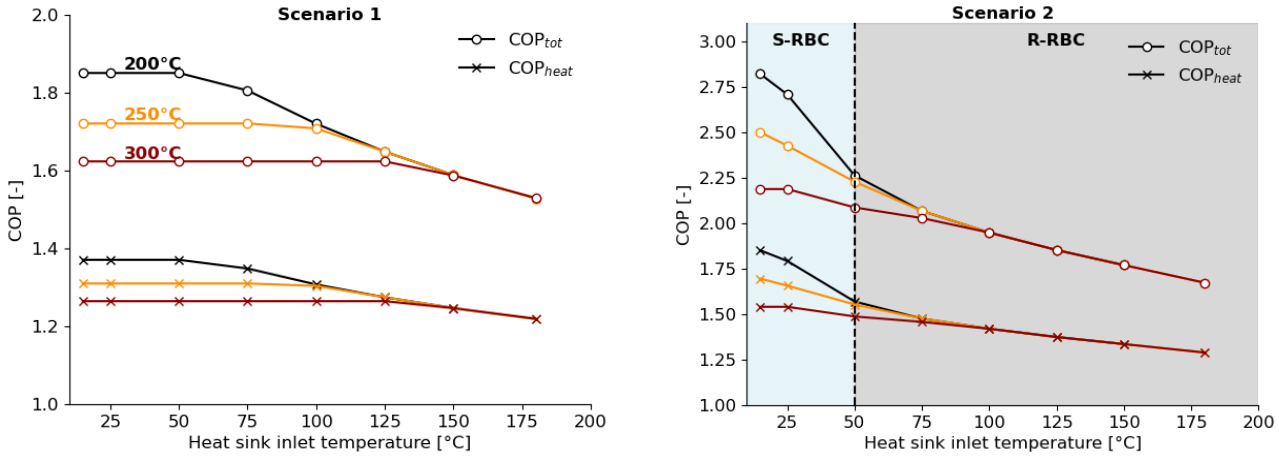

(a) (b)

Figure 3: Heat source inlet temperature of 5 °C (a) and 70 °C (b): Evolution of the heating (cross) and total (circle) COP with the heat sink inlet temperature for supply temperatures of 200 °C (black), 250 °C (orange) and 300 °C (red).

For both scenarios, a general trend is observed: the heating and total COP decrease as the heat sink inlet temperature increases, as shown in Fig. 3. Indeed, this increase leads to an increase in the turbine outlet temperature (TOT), as illustrated in Fig. 4c and 4d, which lowers the available thermal cooling production at the heat source (Fig. 5b). For the first scenario, the recuperated cycle (R-RBC) is identified as the optimal configuration across all operating conditions. For a heat sink outlet temperature of 200 °C, the maximum heating COP ranges from 1.37 to 1.22 while the total COP ranges from 1.85 to 1.53 over the heat sink inlet temperature range considered (from 15°C to 180 °C). At low heat sink inlet temperatures, the system is nearly insensitive to variations in these parameters as the temperatures (Fig. 4a and 4c), mass flow rate and thermal cooling production (Fig. 5, cross markers), and pressure ratio (Fig. 6) remain almost unchanged. Furthermore, the heat sink inlet temperature above

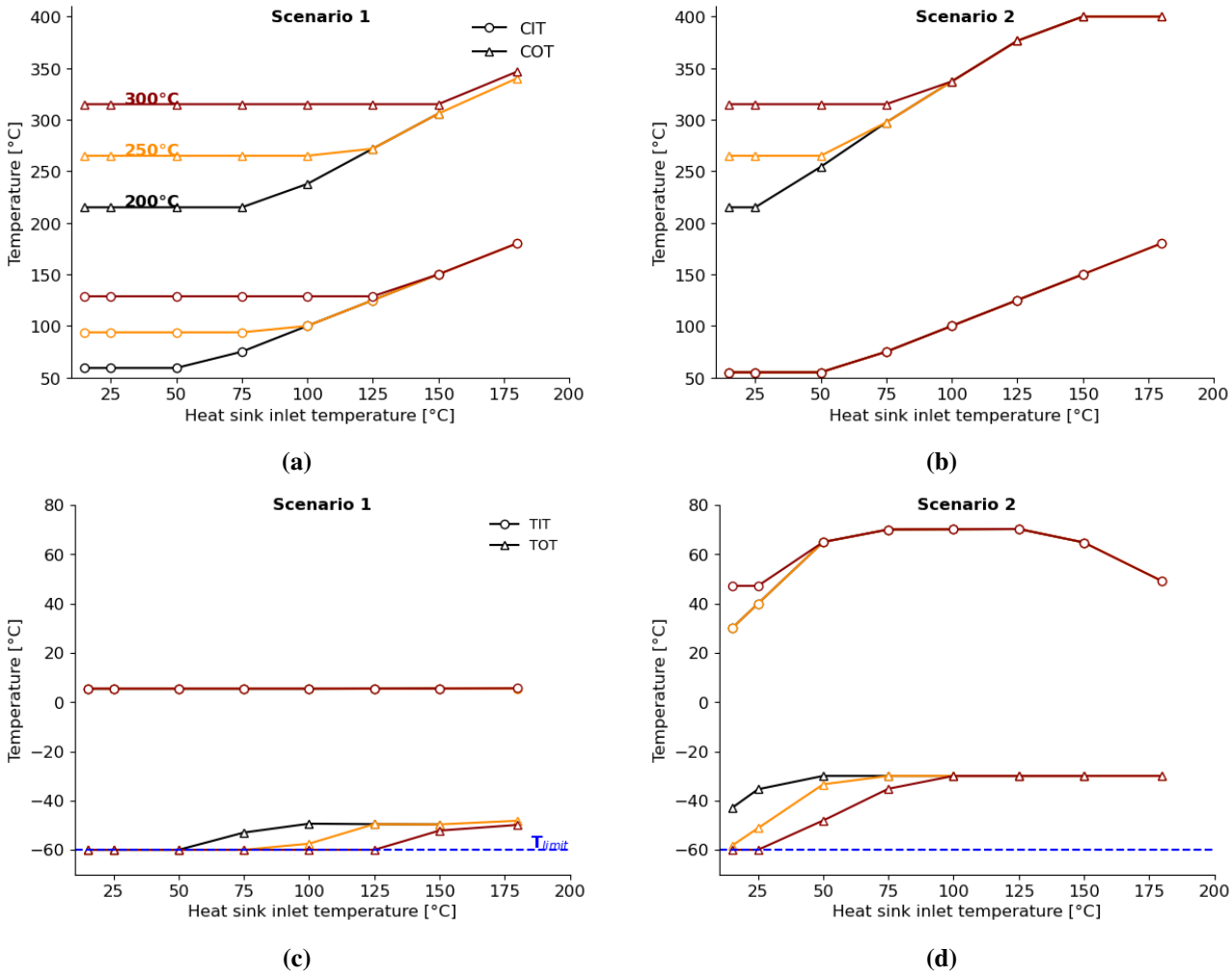

Figure 4: Evolution of the compressor inlet (CIT) and outlet (COT) temperatures (a)-(b) and turbine inlet (TIT) and outlet (TOT) temperatures (c)-(d) with the heat sink inlet temperature. (a)-(c) concerns scenario 1 and (b)-(d) scenario 2.

which the heating and total COPs decrease increases with the heat sink outlet temperature.

For recuperated configuration, increasing the heat sink inlet temperature raises the compressor inlet temperature (CIT), as shown in Fig. 4a. This leads to a reduction in the pressure ratio (Fig. 6, circle markers) and an increase in the TOT (Fig. 4c). When the heat sink inlet temperature reaches 150 °C, all heat sink outlet temperature cases converge to similar COP values (Fig. 3a). This behaviour is associated with a slower decrease in the pressure ratio, as indicated by the change as shown by the change in the slope in Fig. 6 beyond 150 °C. This allows for maintaining a sufficiently low TOT. However, this comes at the expense of a reduced working mass flow rate for temperatures above 125 °C (Fig. 5a, circle markers) and an increase in the compressor outlet temperature (COT), reaching around 300 °C for all heat sink outlet temperatures (Fig. 4a). Thus, all cases converge to the same heating and total COP as the heat pump needs to reach a COT above 300 °C, whatever the heat sink outlet temperature desired. Moreover, for higher heat sink outlet temperatures, the change in the heat sink inlet temperature has a lower impact on the relative decrease of the COP. Indeed, for the total COP and over the full range of heat sink inlet temperature, the drops are equal to -14 %, -11% and -6% for 200 °C, 250 °C and 300 °C, respectively.

For the second scenario, corresponding to the valorisation of waste heat from the industrial process, different behaviours are observed. At a heat sink inlet temperature of 15 °C, heating COP values of 1.85 and 1.54 are obtained for heat sink outlet temperatures of 200 °C and 300 °C, respectively, while the total COP values range from 2.82 to 2.2 (Fig. 3b). In this scenario, the optimal cycle configuration

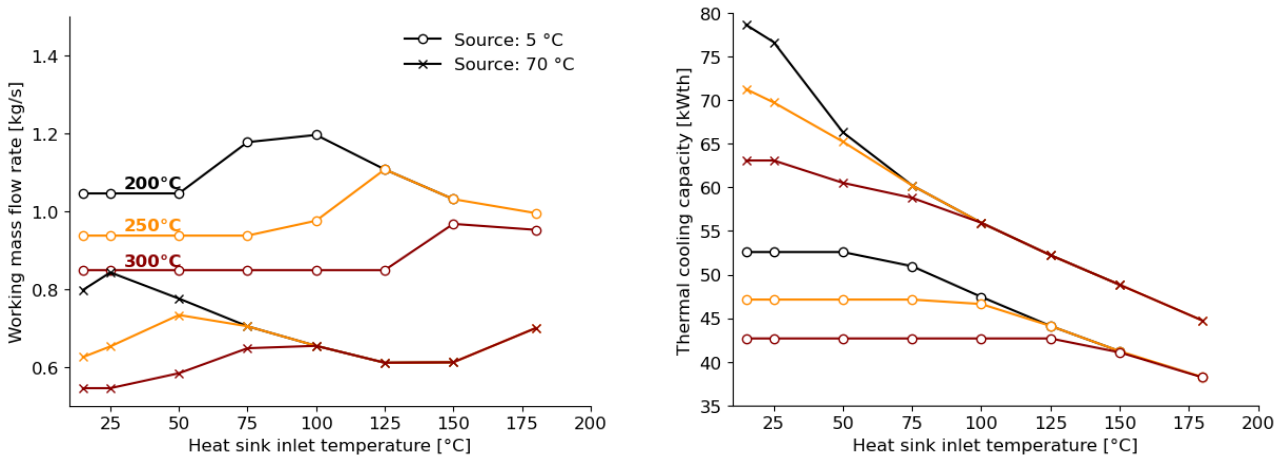

(a) **(b)**

Figure 5: Evolution of the working mass flow rate (a) and thermal cooling power (b) as a function of the heat sink inlet temperature for scenario 1 (circle markers) and scenario 2 (cross markers).

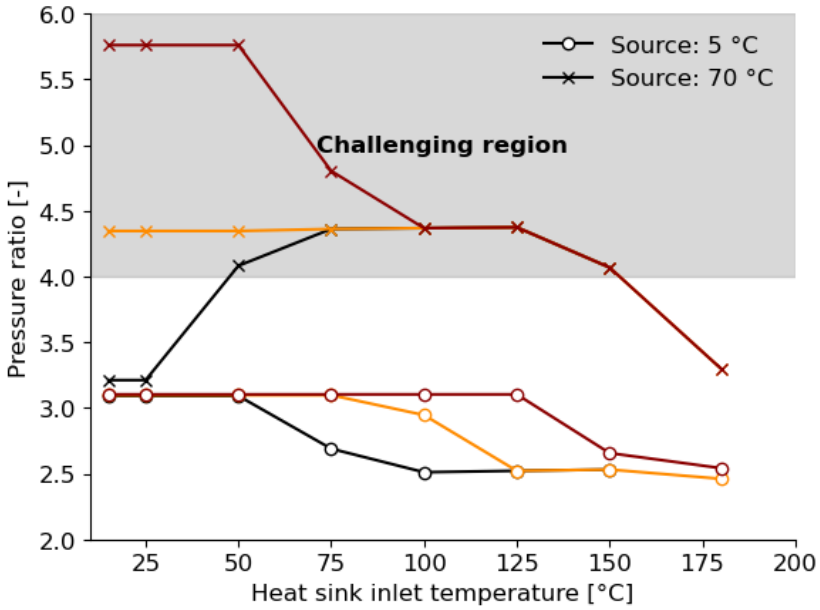

Figure 6: Evolution of the compressor pressure ratio for scenario 1 (circle markers) and scenario 2 (cross markers). Cases with low heat sink inlet temperature, high heat source temperature (cross) are mostly found in the grey area. The latter represents a challenging region for ensuring high compressor isentropic efficiency.

at low heat sink inlet temperatures is no longer the recuperated cycle, but the simple reverse Brayton cycle (S-RBC), as shown in Fig. 1. This occurs when the heat sink inlet temperature is lower than the heat source temperature. Indeed, a higher heat source inlet temperature allows for maintaining a high CIT and reducing compressor work for the same COT. In contrast to scenario 1, the S-RBC exhibits a strong sensitivity to the heat sink inlet temperature, as its COP drops rapidly with the increase of the latter temperature. This is primarily due to the turbine inlet temperature, which, in the absence of a recuperator, varies directly with the heat sink inlet temperature. This drastically increases the TOT (Fig.4d) and consequently reduces the available thermal cooling power (Fig.5b, cross markers).

For a heat sink inlet temperature above 50 °C, the optimal cycle architecture switches back to a recuperated configuration. Similar to the results for scenario 1, after a given heat sink inlet temperature, all curves overlap, indicating that the heat sink outlet temperature no longer influences performance. Furthermore, for a heat sink inlet temperature of 180 °C, the heating COP reaches 1.22 in scenario

1 and 1.29 in scenario 2 for a heat source temperature difference of 65 °C. Over the full range of heat sink inlet temperatures, the total COP decreases by 40 %, 33% and 24% for heat sink outlet temperatures of 200 °C, 250 °C and 300 °C, respectively. While the heat source conditions have a limited impact on COP at high heat sink inlet temperature, they significantly influence internal cycle temperatures. Due to the recuperator and the high heat source inlet temperature, the system tries to keep a low TOT despite the high TIT, which results in a substantial increase in the COT (Fig.4b). For a heat sink inlet temperature of 110 °C, the COT reaches 350 °C, whereas the value is only reached at the highest heat sink inlet temperature (180 °C) in scenario 1. At 180 °C, the COT can reach up to 400 °C (Fig. 4b), while mass flow rate drops below 0.5 kg/s (Fig. 5a). Such high temperatures may increase compressor costs due to the required change of the material to sustain high temperatures.

A large high-temperature glide (¿150°C) and a higher heat source temperature than the heat sink inlet temperature improve heat pump performance and, in some cases, simplify the configuration by eliminating a heat exchanger. In particular, removing the recuperator can significantly reduce the system cost as it is a gas-to-gas heat exchanger.

Finally, beyond the potential high COT around 400 °C, the pressure ratio must also be considered. For radial compressors, maintaining high isentropic efficiency typically becomes challenging for a pressure ratio above 4. As shown in Fig. 6, scenario 1 remains within acceptable limits, with a pressure ratio below 3.1 (circle markers), whereas most cases in scenario 2 lie in the challenging region (grey area). For the S-RBC configuration (15°C to 50 °C of heat sink inlet temperature, cross markers), values up to 5.5 are needed to produce heat at 300 °C. This requirement decreases and falls below 4 when the heat sink inlet temperature is above 150 °C. Consequently, for a low heat sink inlet temperature, two-stage compression may be required to have a feasible system.

4. Conclusion

The objective of this paper was to build a framework to fundamentally characterise Brayton cycle heat pumps for combined heating and cooling production to address the lack of work related to this aspect. To achieve this goal, a MINLP formulation of a single-stage compression and expansion heat pump superstructure model has been used. This simplified model aims to show the potential of the methodology before applying it to more complex configurations.

Therefore, the present cycle was optimised for two different heat source temperatures (5 °C and 70 °C) and three heat sink outlet temperatures (200 °C, 250 °C and 300 °C) while varying the heat sink inlet temperature for a fixed thermal heating power of 150 kW_{th}. For the first scenario with a heat source inlet temperature of 5 °C, the maximum heating and total COP are equal to 1.37 and 1.85, respectively, for a heat sink inlet temperature of 15 °C and a heat supply temperature of 200 °C. For this low heat source inlet temperature, the optimal cycle configuration is the typical recuperated Brayton cycle. On the contrary, when a higher heat source outlet temperature is considered, as soon as the heat sink inlet temperature is lower than the previous temperature, the optimal architecture is the simple Brayton cycle. The latter achieves heating and total COP up to 1.85 and 2.82 for the same heat sink conditions considered earlier. Such a system has the advantage of reducing the cost of the system as it does not need a recuperator, which is a gas-to-gas heat exchanger. For both scenarios, the COPs trend shows a decrease with the increase of the heat sink inlet and outlet temperatures due to the influence on the pressure ratio, turbine outlet temperature and thus the valorisation of the thermal cooling produced. To compensate for this decrease, the systems decrease the working mass flow rate and increase the compressor outlet temperature to ensure a high thermal cooling production at the desired outlet temperature of -15 °C. Furthermore, although a higher heat source inlet temperature can increase the heat pump performance, its effects diminish with the increase of the heat sink inlet temperature, implying that the recovery of high-temperature waste heat may be unnecessary. In addition,

for a higher heat source inlet temperature, most considered cases require a compressor pressure ratio from 4 to 5.5, which lies in the region where maintaining high-isentropic efficiencies is challenging.

In future work, the superstructure model of the heat pump can be improved to integrate more compressors and turbines to have the possibility of inter-cooling or inter-heating. In addition, multiple sinks and sources could also be implemented with the possibility for direct heat recovery between sink and source streams. Finally, the objective function can be integrated with economic correlations while also looking at the footprint of the heat pump and compared with other technologies, such as the vapour compression cycle.

Acknowledgments

Christophe Vankelekom is a Research Fellow of the Fonds de la Recherche Scientifique – FNRS.

Nomenclature

CIT Compressor Inlet Temperature
COP Coefficient of Performance
COT Compressor Outlet Temperature
RBC Reverse Brayton Cycle
TIT Turbine Inlet Temperature
TOT Turbine Outlet Temperature
F Surrogate model function
i Index for hot stream
j Index for cold stream
k Index for stage-wise superstructure stage
h enthalpy, $\mathrm{J/kg}$
$\dot{m}$ mass flow rate, $\mathrm{kg/s}$
P Power, W
Q Heat duty, W
T temperature, $^{\circ}\mathrm{C}$
Z Binary number accounting for the hot and cold stream matches

Greek symbols

π Pressure ratio

Subscripts and superscripts

c Cold
comp Compressor
h Hot
turb Turbine

References

[1] de Boer R., Marina A., Zühlsdorf B., Arpagaus C., Bantle M., Wilk V., Elmegaard B., Corberán J., Benson J. *Strengthening industrial heat pump innovation: Decarbonizing industrial heat*. 2020.

[2] Philibert C. *Renewable energy for industry*. Paris: International Energy Agency; 2017.

[3] Zühlsdorf B. *High-Temperature Heat Pumps: Task 1–Technologies. Annex 58 about High-Temperature Heat Pump*. Heat Pump Center c/o RISE; 2023.

[4] Ossorio R., Navarro-Peris E., Barta R.B. *Impact of lubricant in the performance of variable speed heat pumps working with R290*. International Journal of Refrigeration 2023;145:436-45.

[5] Yoo J., Estrada-Perez C.E., Choi B.-H. *Investigation of heat pump technologies for high-temperature applications above 250° C*. Applied Energy 2025;384:125384.

[6] Zühlsdorf B., Bühler F., Bantle M., Elmegaard B. *Analysis of technologies and potentials for heat pump-based process heat supply above 150 C*. Energy Conversion and Management: X 2019;2:100011.

[7] Shuailing L., Ma G., Xu S., Gong Y., Jia X., Wu G. *A review of reverse Brayton air cycle refrigerators*. International Journal of Refrigeration 2023;150:200-14.

[8] Pimm A.J., Cockerill T.T., Gale W.F. *Reducing industrial hydrogen demand through preheating with very high temperature heat pumps*. Applied Energy 2023;347.

[9] Jende E., Kabat N., Stathopoulos P., Nicke E. *Thermodynamic analysis of an industrial process integration of a reversed Brayton high-temperature heat pump: A case study of an industrial food process*. In: E3S Web of Conferences; 2023;414:03006.

[10] Rehfeldt M., Fleiter T., Toro F. *A bottom-up estimation of the heating and cooling demand in European industry*. Energy Efficiency 2018;11(5):1057-82.

[11] Marina A., Spoelstra S., Zondag H.A., Wemmers A.K. *An estimation of the European industrial heat pump market potential*. Renewable and Sustainable Energy Reviews 2021;139:110545.

[12] Kabat N., Jende E., Nicke E., Stathopoulos P. *Investigation on Process Architectures for High-Temperature Heat Pumps Based on a Reversed Brayton Cycle*. In: Turbo Expo: Power for Land, Sea, and Air; 2023;86984:V005T06A015.

[13] Yücel F.C., Oehler J., Kriese M., Jende E., Setzepfand N., Stathopoulos P. *Design and Commissioning of the Brayton High-Temperature Heat Pump "Cobra"*. Available at: SSRN 5290358.

[14] Padullés R., Walmsley T.G., Andersen M.P., Elmegaard B. *Pinch design method for heat exchanger networks with optimal heat pump selection*. Applied Thermal Engineering 2025:128506.

[15] Wallerand A.S., Kermani M., Kantor I., Maréchal F. *Optimal heat pump integration in industrial processes*. Applied Energy 2018;219:68-92.

[16] Yee T.F., Grossmann I.E. *Simultaneous optimization models for heat integration—II. Heat exchanger network synthesis*. Computers & Chemical Engineering 1990;14(10):1165-84.

[17] Linnhoff B., Flower J.R. *Synthesis of heat exchanger networks: I. Systematic generation of energy optimal networks*. AIChE Journal 1978;24(4):633-42.

[18] Aspen Technology, Inc. *Aspen Plus: Leading Process Simulation Software*. Available at: `https://www.aspentech.com/en/products/engineering/aspen-plus` [accessed 27.3.2026].

[19] Andersson J.A.E., Gillis J., Horn G., Rawlings J.B., Diehl M. *CasADi — A software framework for nonlinear optimization and optimal control*. Mathematical Programming Computation 2019;11(1):1-36.

[20] Wächter A., Biegler L.T. *On the implementation of an interior-point filter line-search algorithm for large-scale nonlinear programming*. Mathematical Programming 2006;106(1):25-57.

[21] De Paepe W., Delattin F., Bram S., De Ruyck J. *Water injection in a micro gas turbine–Assessment of the performance using a black box method*. Applied Energy 2013;112:1291-302.